

Experimental tests and global modeling of masonry infilled frames

Alessandro Vittorio Bergami* and Camillo Nuti^a

University of Roma Tre, Department of Architecture, Largo G. B. Marzi 10, Rome, Italy

(Received March 27, 2014, Revised April 1, 2015, Accepted April 6, 2015)

Abstract. The effects of infill panels on the response of r.c. frames subjected to seismic action are widely recognized. Numerous experimental investigations were effected and several analytical models were developed on this subject. This work, which is part of a larger project dealing with specific materials and structures commonly used in Italy, discusses experimental tests on masonry and samples of bare and infilled portals. The experimental activity includes tests on elemental materials, and 12 wall samples. Finally, three one-bay one-story reinforced concrete frames, designed according to the outdated Italian technical code D.M. 1996 without seismic details, were tested (bare and infilled) under constant vertical and cyclic lateral load. The first cracks observed on the framed walls occurred at a drift of about 0.3%, reaching its maximum capacity at a drift of 0.5% while retaining its capacity up to a drift of 0.6%. Infill contributed to both the stiffness and strength of the bare reinforced concrete frame at small drifts thus improving overall system behavior. In addition to the experimental activities, previously mentioned, the recalibration of a model proposed by Comberscue (1996) was evaluated. The accuracy of an OpenSees non linear fiber based model of the prototype tested, including a strut element was verified through a comparison with the final experimental results. This work has been partially supported by research grant DPC-ReLUIIS 2014.

Keywords: seismic response; infilled frames; masonry; cyclic test

1. Introduction

Masonry infilled framed structures were traditionally designed without taking into account the presence of infills, except for their gravity load. This commonly accepted design process, due also to the lack of available reliable models, led to a simplified structural analysis.

In reality, especially under horizontal loads, the influence of the infills could cause important changes in both static and dynamic structural response. It is well known that infills influence the extent of the structure's stiffness and its distribution both in plan and elevation. Furthermore, as well demonstrated by experimental studies (Colangelo 2005) and experiences from past seismic events, they also influence the distribution of forces on structural elements (e.g., shear increase on columns adjacent to infills or short column effects in case of non continuous column-infill interface). In particular, when damage or serviceability limit states are considered, the effects of

*Corresponding author, Ph.D., E-mail: alessandro.bergami@uniroma3.it

^aProfessor, E-mail: camillo.nuti@uniroma3.it

the infills are dominant and the ductility of the bare frame plays a minor role in the response. In fact under seismic action the first damage usually happens on the infill panels due to their fragile behavior whereas the structure is still in the elastic range but, if the panels damage limit isn't reached, a global reduction of interstorey drift may occur (the infilled frame is stiffer than the bare one, if the infills are well distributed) and therefore building performance may benefit. Moreover, particularly with regard to the collapse limit state, another beneficial effect from the presence of infills is represented by a significant increase of maximum resistance to horizontal load.

At any rate, in common practice, only negative consequences (e.g., irregular distribution of stiffness, soft storey, short column effects) are considered whereas its structural contribution to strength can't be evaluated because infills are realized with a masonry that isn't a structural material with formally defined mechanical characteristics; for this reason the walls should be completely disconnected from the structural frame so as not to alter the behavior expected from a standard design process.

A great deal of research activity, both numerical and experimental, was devoted, during the past 50 years, to investigate the seismic response of infilled reinforced concrete frames and design rules and recommendations have been developed for this type of widely diffused structures. Recent earthquakes (e.g., L'Aquila, Italy - 2009) have shown the significance of this topic at the present time, both for existing and new constructions. The importance of the so called "non structural" elements in governing the global seismic response and the corresponding level of safety against collapse has been highlighted many times (Fardis *et al.* 1999).

These results demonstrate the need to define a simple and quick method, to be used by professional engineers to implement the contribution offered by infills: therefore in this paper an experimental course covering materials and samples of masonry infilled r.c. frames will be taken to evaluate a simple approach.

According to scientific literature and technical code indications two modeling approaches can be used to analyze masonry infilled frames: global and local. In the local approach, each part (the frame and the infill panels) is discretized and the hypothesis made for the contact between the frame and the infill panels becomes important since global stiffness is highly dependent on the presence of cracks at this interface. In the global approach, that is used in this study, each masonry panel is often replaced by trusses with a uniaxial behavior law. The complexity of the behavior depends on the various phenomena that is taken into account by the model (pinching due to crack closure, crushing of masonry at the corners, decrease of stiffness due to cracking, etc.). The frame is modeled by beam and column elements with moment curvature relationships or fiber type models. This approach allows a large number of computations with dynamic or cyclic loading but the identification of the truss parameters is often based on empirical rules. When there is a modification in the panel characteristics, the validity limit of the formulae used may be reached: that is why in this study activities started with the execution of experimental tests on masonry. Moreover studies have shown that the wall itself can develop many different failure modes (shear sliding along an horizontal bed joint, diagonal tensile failure, crushing at the diagonal struts).

This paper describes the experimental activities performed at the Laboratory for experiments on materials and structures located at the University of Roma Tre, to evaluate the seismic response of r.c. frames infilled with a masonry that is widely used in Italy: a more detailed description of the entire experimental course is in Bergami (2011). The experimental activity will be described, thus providing a detailed data base for further studies, following the chronological sequence of the experimental course: tests on materials, walls, portal frames and a numerical analysis. At a later stage the experimental course will be used to evaluate a global approach for the definition of

numerical models of r.c. infilled frames, providing useful indication to designers.

2. Experimental activity on masonry

2.1 Experimental activity on masonry units and mortar

When using global models, the sensitivity to the masonry adopted is strong. Therefore, in order to well identify the typology of masonry considered, this study started with the execution of experimental tests on masonry.

The experimental activity on masonry deals with the characterization of each single component used later to make wall samples and infill the frame prototypes. The starting point was therefore a careful selection of bricks and mortar used to realize twelve wall samples (the characteristics of the selected bricks and mortar were identified with specific experimental tests). On the wall samples, after 28 days of ripening, vertical, horizontal and diagonal compression tests were performed. The mortar selected is one of those preferred in Italy: it is a pre-mix mortar consisting of hydrated lime, Portland cement, sand and chemical additives to reduce the setting time.

- specific weight in powder 1500 kg/cm³
- granulometry <3 mm
- minimum thickness 10 mm
- paste water 18%
- elastic modulus after 28 days 8000 Mpa (data from factory)
- class M5 (according to UNI EN998-2 indications)

The bricks used (Fig. 1) were chosen because they are widely used in Italy: half-full bricks (12×12×25 cm³) with vertical holes (definitions provided by Italian masonry Code D.M. LL.PP. 20.11.1987).

To determine the mortar's mechanical properties, the following tests were performed in accordance with UNI EN 1015-11 requirements:

- bending tests on three points (on prismatic samples of mortar) to evaluate the traction strength $f_{ctk}=3.08$ MPa
- compression tests on cylindrical samples to evaluate the average values of compressive strength $f_m=11.72$ MPa and elastic modulus $E_m=16961$ MPa

2.2 Experimental tests on wall samples

The wall specimens were built using the bricks and mortar described in the previous paragraph. All of the walls (12 specimens) were built by an expert construction worker. The construction's accuracy level is comparable to the procedures commonly used on building sites and features



Fig. 1 Half-full bricks 12×12×25 cm³

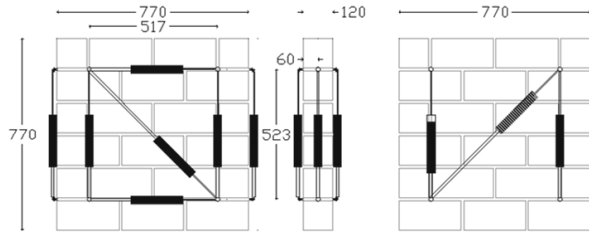


Fig. 2 Layout of wall sensors compressed parallel or orthogonally to holes [mm]

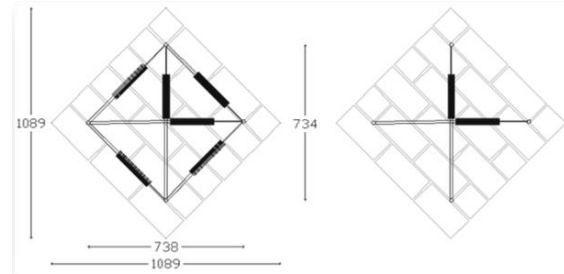


Fig. 3 Layout of wall sensors compressed diagonally [mm]

constant bed-joints with a thickness of approximately 10 mm. After 28 days the samples were subjected to compression tests; of the twelve samples four were loaded parallel to the holes, four orthogonally to the holes and four were loaded diagonally.

F_v and F_h represent the maximum gravity load applied during the test (vertical or horizontal) and t , l and h the thickness, length and height of the walls.

The compression strength in the vertical f_{wv} and horizontal f_{wh} direction have been calculated as follows

$$f_{wv} = F_v / (l \cdot t) \quad (1)$$

$$f_{wh} = F_h / (h \cdot t) \quad (2)$$

The shear strength f_{wd} was determined from diagonal compression tests as the average value of the tangential stress, acting parallel to the sides of the wall, corresponding to maximum load F_d according to ASTM E519-81 standards Eq. (3). In the following equation, the symbols E_v , E_h and E_d will be used to indicate vertical, horizontal and diagonal elastic modules while G_w is the shear module (being ε_{w1} and ε_{w2} the strains parallel and orthogonal to load direction)

$$f_{wd} = F_d / (\sqrt{2} \cdot l \cdot t) \quad (3)$$

$$G_w = f_{wd} / \gamma_w \quad (4)$$

$$\gamma_w = \frac{\varepsilon_{w1} - \varepsilon_{w2}}{2} \quad (5)$$

Figs. 4, 5 and 6 illustrate, for example, some samples during the compression tests and the stress-strain curves obtained from all samples are plotted. Both vertical (parallel to holes) and horizontal (orthogonal to holes) compression tests highlight an elastic behavior with a brittle failure and low residual strength. Furthermore it is clear that in the main loading directions (vertical and horizontal), deformations towards collapse can be compared while the maximum load achieved differs approximately 60%: the strongest direction is parallel to the holes. Differently from orthogonal to holes compression tests, parallel and diagonal tests show evidence of scattering: this is probably related, for the former, to a higher sensitivity to the wall planar configuration as the loading force is significantly stronger and, for the latter, to the unavoidable imperfection of the contact surface between the angular plate and the wall.

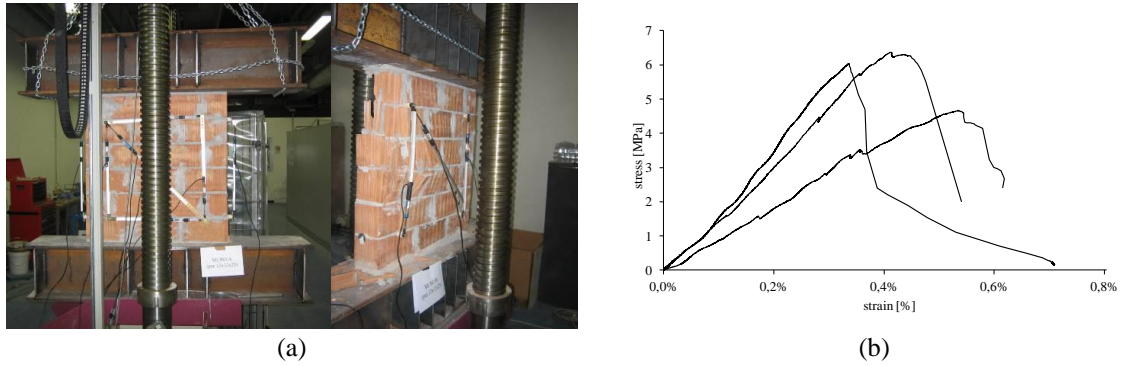


Fig. 4 (a) compression test parallel to holes, initial phase and collapse; (b) compression tests parallel to holes, stress-strain curves

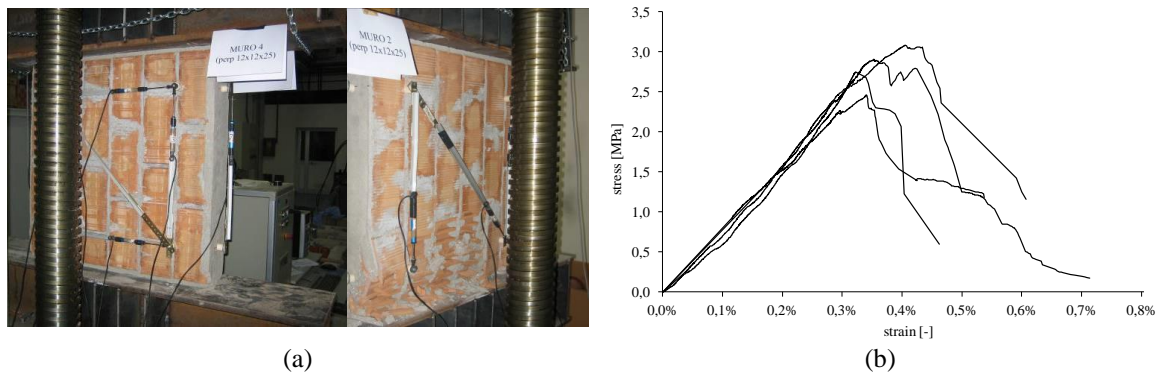


Fig. 5 (a) compression test orthogonal to holes, initial phase and collapse; (b) compression tests orthogonal to holes, stress-strain curves

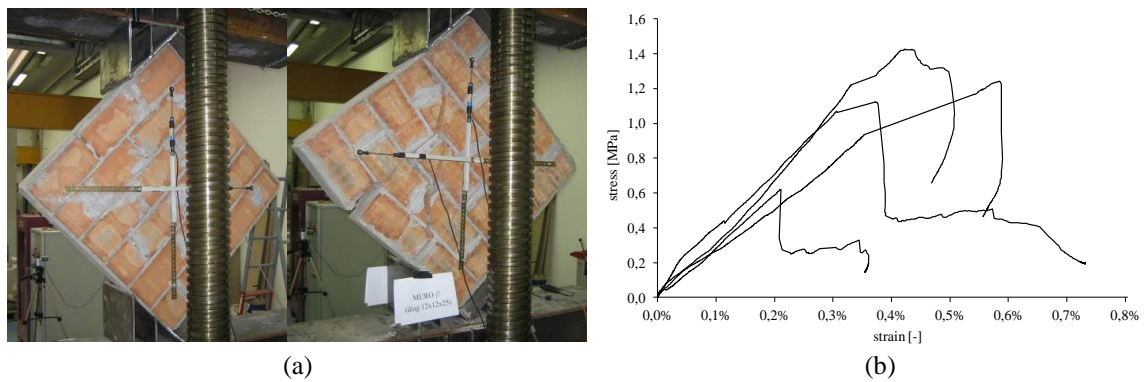


Fig. 6 (a) diagonal compression test, initial phase and collapse; (b) diagonal compression tests, stress-strain curves

In diagonal compression tests the failure occurs due to the diffusion of two parallel cracks that delimited a central compressed strut and the consequent detachment of one of the free corners. Tables 1, 2, 3 illustrate results from compression tests on walls in the three loading directions: the

Table 1 Results of compression tests on walls with load parallel to holes

<i>Sample</i>	<i>F</i> [kN]	<i>f_{wv}</i> [MPa]	<i>ε_v</i>	<i>E_v</i> [MPa]
1	431,02	4,66	0,53%	871,54
2	557,46	6,03	0,33%	1796,33
3	588,38	6,36	0,41%	1539,25
4			test failed	
Average	489,04	5,29	0,38%	1402,37
Average reliable samples: 2,3	572,92	6.19	0,37%	1667.67

Table 2 results of compression tests on walls with load orthogonal to holes

<i>Sample</i>	<i>F</i> [kN]	<i>f_{wh}</i> [MPa]	<i>ε_h</i>	<i>E_h</i> [MPa]
1	186,23	2,01	0,166%	749,20
2	268,58	2,90	0,353%	1900,72
3	284,95	3,08	0,405%	1875,01
4	254,13	2,75	0,322%	1387,97
Average	208,53	2,68	0,31%	1478,23
Average reliable samples: 2,3,4	269,22	2,91	0,36%	1721,233

Table 3 results of diagonal compression tests on walls

<i>Sample</i>	<i>F</i> [kN]	<i>f_{wd}</i> [MPa]	<i>ε_d</i>	<i>E_d</i> [MPa]
1	162,28	1,24	0,58%	244,41
2	186,28	1,42	0,42%	366,98
3	146,89	1,12	0,37%	291,14
4	80,78	0,61	0,21%	303,57
Average	144,05	1,09	0,39%	301,52
Average reliable samples: 1,2,3	165,15	1,26	0,45%	300,8433

Table 4 elastic modulus determined from internal transducers

<i>Parallel load</i>		<i>Orthogonal load</i>		<i>Diagonal load</i>	
<i>Sample</i>	<i>E_v</i> [MPa]	<i>Sample</i>	<i>E_h</i> [MPa]	<i>Sample</i>	<i>E_d</i> [MPa]
1	3425	1	2340	1	2865
2	5757	2	5291	2	5442
3	8699	3	4237	3	3788
4	failed	4	3889	4	2389
Average	7228	Average	4472	Average	4031

maximum applied load F and the corresponding strength f_w , elastic modulus E (determined referring to the press excursion) and relative average values. For a more accurate evaluation of the

elastic modulus, another calculation was made with transducers installed on the wall (internal transducers, Figs. 2-3). Table 4 evidences that the values are higher than those obtained referring to the displacement of the press plate; analysis have been performed according to values of Tables 1, 2, 3 in order to evaluate the behaviour of a panel including boundary effect also (the infill wall is realized after that the frame has been completed and therefore vertical and higher joints, in common practice, are filled up with unloaded mortar: this strongly reduces stiffness).

Tables 1, 2, 3 illustrate the global average value of the compressive strength, and considers only reliable samples (Table 1-samples 2, 3; Table 2-samples 2, 3, 4; Table 3-samples 1, 2, 3), whereas f_w =average (f_{wv} , f_{wh} , f_{wd})=3.37 MPa: only tests not influenced by external causes (e.g., panel not well realized or damaged during the installation on the experimental apparatus), have been considered reliable.

3. Description of the r.c. portal frame prototype

Specimens represent the first floor of a three-story building (Fig. 7) whose structure may be classified as a regular frame system (regularity as defined by Eurocode). Essentially it is assumed that a single horizontal seismic force acts in the middle of the beam, where the seismic displacement is imposed. Gravity load is considered to be a vertical force applied on the beam-column joint. Each force coming from the three stories amounts to 159 kN. Obviously, the actual stress on the joint is disregarded, and confinement by transverse beams is omitted. Based on such observations, a decision was made to exclude unrealistic joint failure with additional hoops, and to focus on the member's behavior. Both beam and column longitudinal bars are anchored around the joint core with a single bent. To simplify, the frame represents previous structures made with columns that were not designed to withstand any horizontal action. Column and beam reinforcement is dictated by Italian non-seismic provisions (D.M. LL.PP. 9.01.1996). Non-structural, unreinforced masonry infill is built in contact with the frame, without any connector; mortar forms both a head and bed joint, and the infill surface is not plastered for rendering. Due to the impossibility of scaling commercial masonry bricks it was decided to build the portals in a 1:2 scale ratio on the portal plane, and in a 1:1 scale ratio in the orthogonal direction (to maintain the real depth of columns and beam); to reduce errors as much as possible, the smallest bricks available on market were chosen (scale factors are shown in Table 5). Fig. 8 illustrates the structural details of the prototype sample.

3.1 Experimental activity on portals

Cyclic tests (in displacement control) up to collapse (the collapse state considered as the lost of stability of the r.c. frame) were performed on the three portal prototypes, realized as previously

Table 5 portal frame sample scale ratios

<i>Characteristic</i>	<i>Scale ratio</i>
<i>Thickness, tension, elastic modulus, stiffness</i>	1:1
<i>Height, length, movement</i>	1:2
<i>Diameter of the bars</i>	1: $\sqrt{2}$
<i>Bending moment</i>	1:4

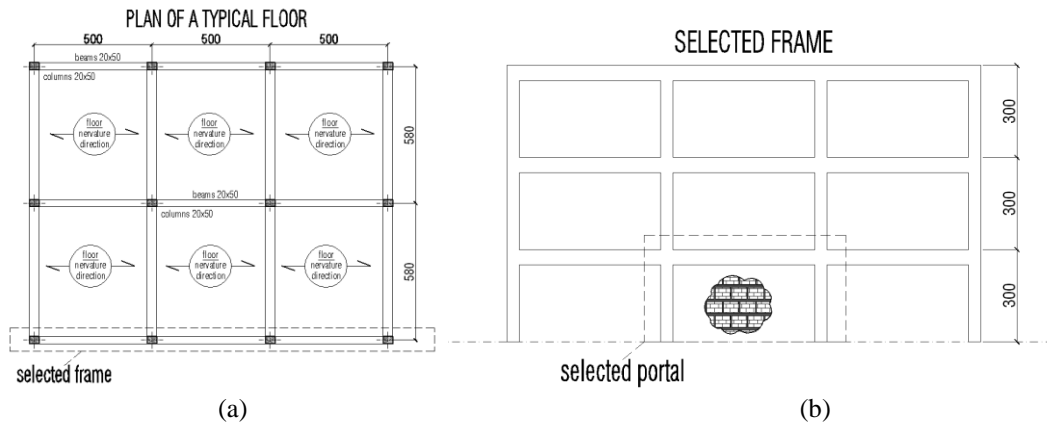


Fig. 7 (a) planar view of the building containing the frame under examination (scale ratio 1:1, length in [cm], the frame is highlighted); (b) the frame analyzed (scale ratio 1:1), the position of the portal (realized in a reduced scale ratio) is highlighted [cm]

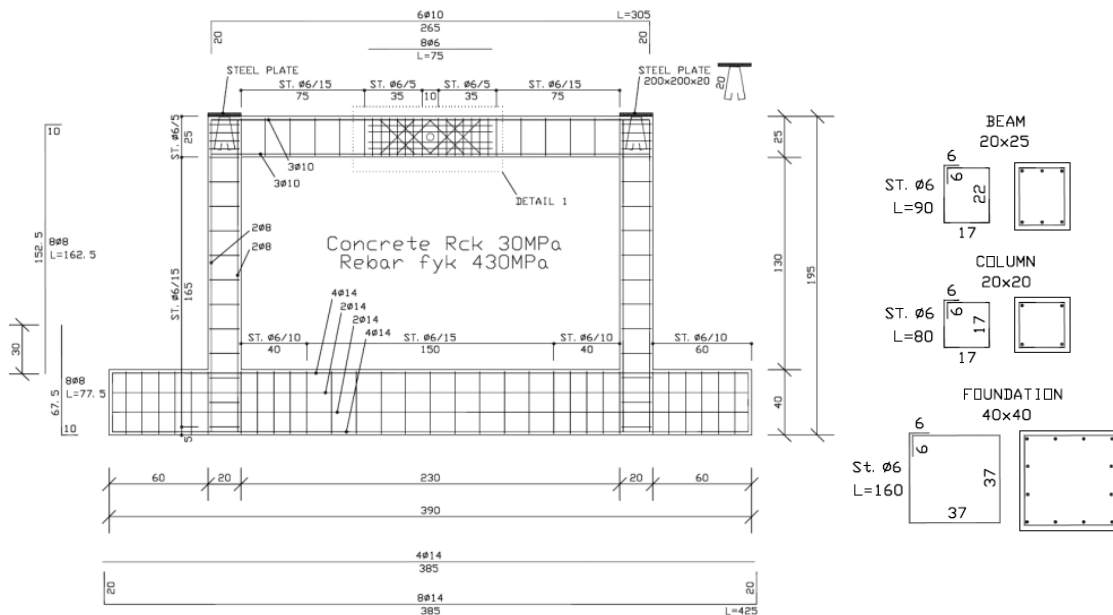


Fig. 8 Prototype characteristics

described: the first test was performed on the bare portal (F_{n1}) and the other two on portals infilled with the previously described masonry and tested (F_{i1} , F_{i2}).

The experimental equipment and results are described here under; it is important to point out that, with regard to portal F_{i1} , only partial results are provided because some data was lost due to technical problems. The experimental apparatus for the execution of the cyclic tests includes the following elements:

- a hydraulic jack for horizontal load M_h (to impress the cycles);

- a hydraulic jack for gravity load M_v (to simulate vertical loads from higher levels);
- displacement transducers;
- a loading cell (to monitor vertical load);
- vertical and horizontal locking systems (to fasten foundations to the laboratory floor);
- connections between the portal and the jack M_h .

In Fig. 9 the developed test system and an image of portal F_{n1} are illustrated.

As previously mentioned, cyclic tests were carried out applying a gravity load of 159 kN (the force coming from three stories of the scaled case study amounts to 159 kN) on each beam-column joint. Regularly, during test execution, the crack patterns were tagged with a marker. The portal F_{n1} , as illustrated in Fig. 10, was fitted with the following instruments:

- 24 displacement transducers positioned in the plastic hinge areas of columns and beams;
- 5 displacement transducers between a column and a metal structure firmly attached to the basement;
- 1 transducer between the edge of the jack and the portal itself (this instrument allows measurement of the relative displacement caused by strain on the linking elements or imperfections)
- 1 transducer applied on the M_h jack to verify the excursion of the piston, through use of an external instrument.

As illustrated in Fig. 11, in addition to the same transducers used for the portal F_{n1} , the following transducers were also installed on infilled portals F_{i1} and F_{i2} :

- 6 displacement transducers positioned on the interface between the wall and the columns;
- 1 displacement transducer positioned on the interface between the wall and the center of the beam;
- 8 transducers positioned along the two diagonal wall lines ;
- 2 transducers diagonally connecting the nodes of the portal frame.

All cyclic tests performed (both on bare and infilled portals) imposed displacement histories having the following characteristics (Fig. 12):

- magnitude of the first imposed cycle 1 mm ($\pm 0,5$ mm);

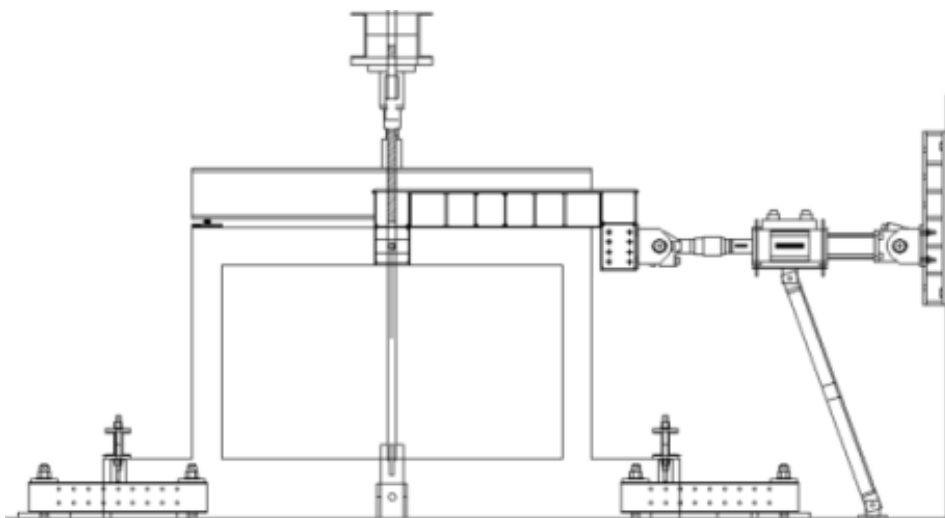


Fig. 9 Layout of the developed test system

- 3 cycles for each magnitude step;
- magnitude increases by ± 0.5 mm up to the achievement of the maximum strength and subsequent increases are ± 1.0 mm;
- cycles with a constant frequency of 0.05 Hz.

During each test execution, jack thrust was systematically suspended, at regular intervals. This made it possible to identify developing cracks on the concrete and masonry.

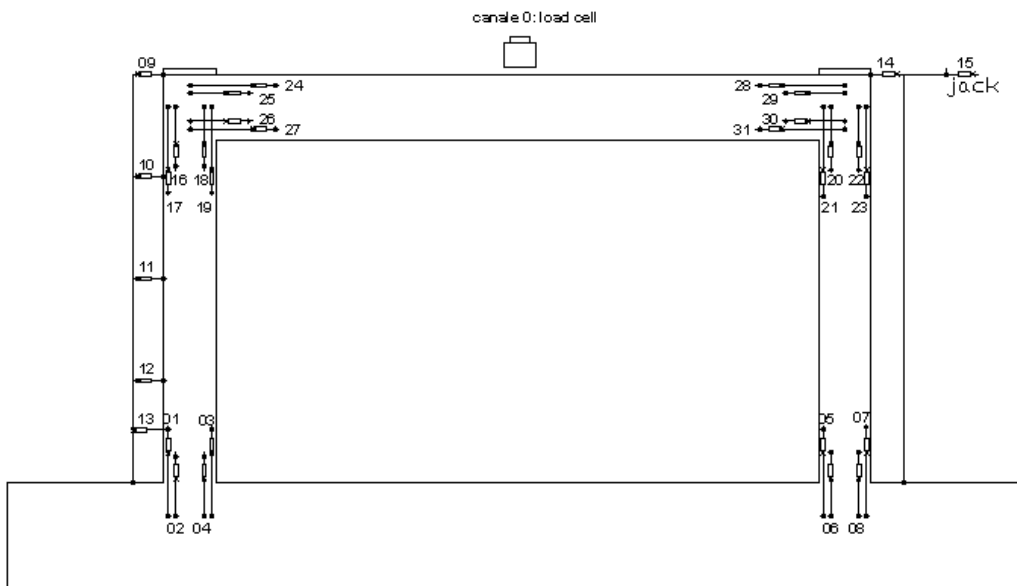


Fig. 10 Instrumentation of the bare portal

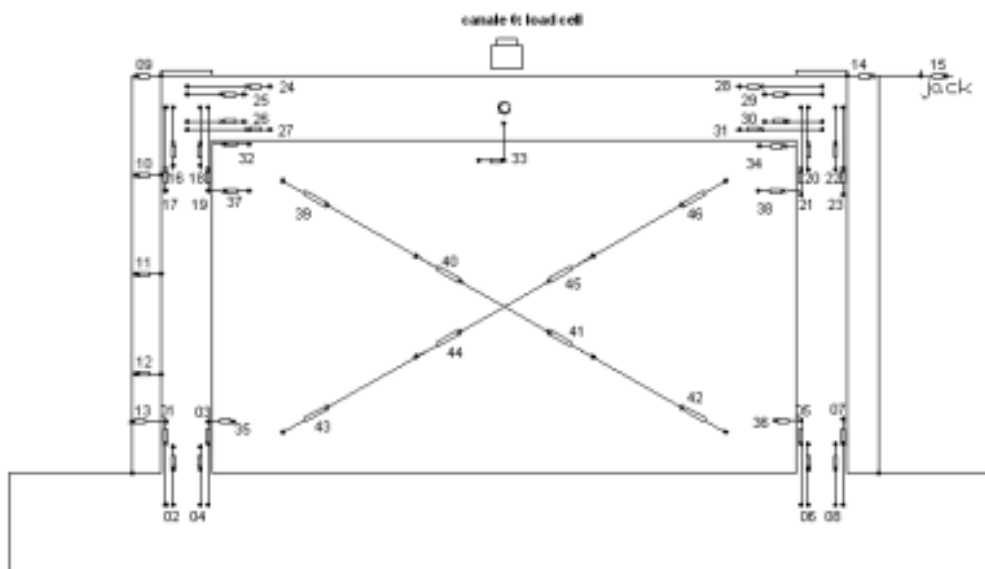


Fig. 11 Instrumentation of the infilled portal

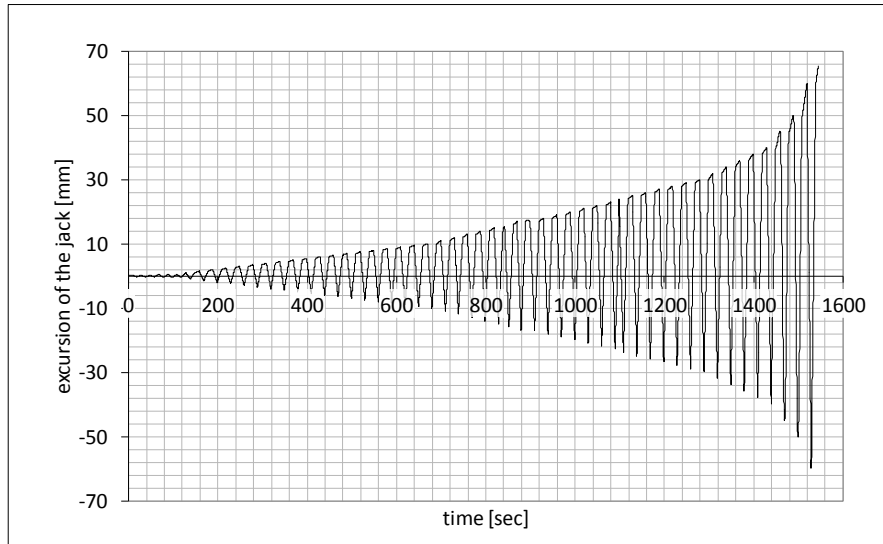


Fig. 12 displacement history imposed during the tests: n time-horizontal excursion of the jack [sec, mm]

3.2 Results from experimental tests on the bare portal F_{n1}

The first plastic hinges were developed at the base of the columns in correspondence with an imposed top displacement of 4.33 mm, corresponding to an interstory drift of 0.17%.

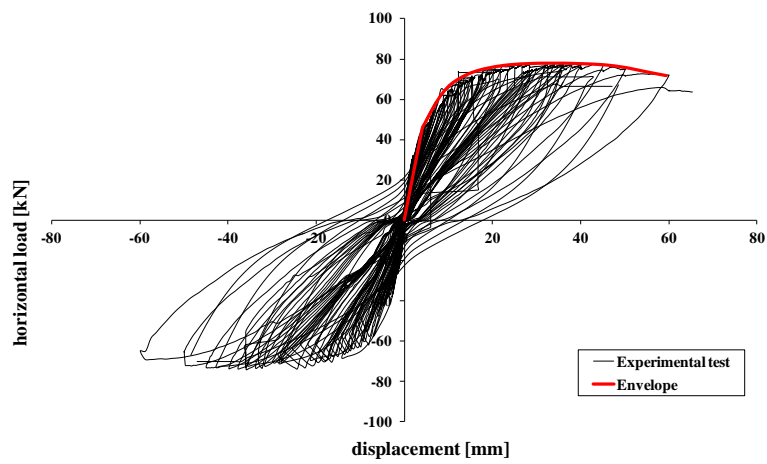
The sequence of damage observed follow: cracks on the base of the columns became increasingly apparent as the amplitude of the cycles increased and, for a top displacement of 8.63 mm (corresponding to an interstory drift of 0.34%), other cracks appeared in correspondence to the upper column extremities. Once the top displacement exceeded 15 mm (with a 0.6 % interstory drift) the lower sections of the columns were strongly damaged and the concrete cover started to be expelled by the compressed, buckled rebars. Once a top displacement of approximately 20 mm was achieved the structure reached its maximum resistance and the subsequent increase of displacement corresponded to a substantially constant load; the test was interrupted when a top displacement of 60 mm was achieved. Fig. 13 illustrates the final condition of the sample at test conclusion.

When the extremities of the columns were all severely damaged, but no mechanism was noticeable on the beam (strong beam and weak columns).

Figs. 14-15 illustrates how, in the upper sections of the columns, the concrete cover was also expelled on the internal side of the portal: in the bottom sections the bars buckled and the concrete cover was expelled in correspondence with the overlapping basement rebars, symmetrically on both sides of each column.

In Figs. 16-17 the experimental results achieved are illustrated in terms of top displacement (transducer 9; see Fig. 10)-horizontal load and curvature-horizontal load: the presence of some anomalous vertical lines is a consequence of the impact between the instruments and some falling material.

All main parameters, estimated by the experimental test, are summarized in Table 6 (yielding=yielding of the first rebar in whichever r.c. section, collapse=reduction of resistance to horizontal load greater than 50% of the maximum load achieved).

Fig. 13 Portal F_{n1} , final crack pattern (test concluded)Fig. 14 Portal F_{n1} , damage at lower extremities of columns (test concluded)Fig. 15 Portal F_{n1} , damage at the upper extremities of columns (test concluded)Fig. 16 Portal F_{n1} , top displacement-horizontal load

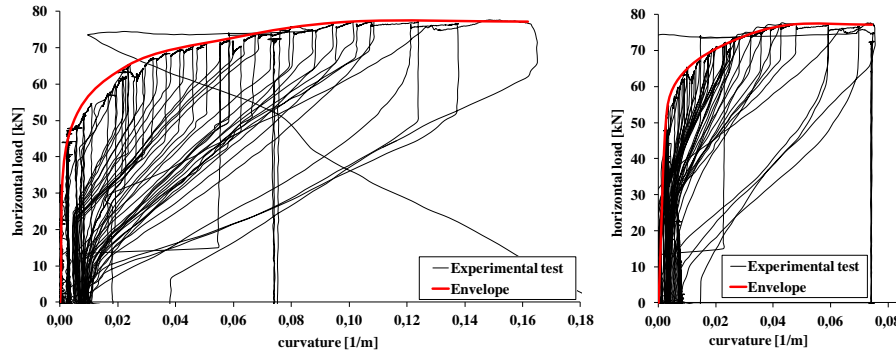


Fig. 17 Portal F_{n1} column curvature-horizontal load, (a) lower section (b) upper section

Table 6 main parameters from experimental test on portal F_{n1}

$K_{1,n1}$	12300	kN/m	Elastic stiffness
$K_{2,n1}$	2230	kN/m	Post-elastic stiffness
$F_{max,n1}$	77.3	kN	Maximum horizontal load achieved
$F_{y,n1}$	45.0	kN	Horizontal load at yielding of the first rebar
$\delta_{y,n1}$	4.2	mm	Horizontal displacement at yielding of the first rebar
$\delta_{u,n1}$	60	mm	Horizontal displacement at collapse (lack of resistance to horizontal load)
$\theta_{yinf,n1}$	0.00538	1/m	Column lower section: curvature in correspondence with $F_{y,n1}$
$\theta_{ysup,n1}$	0.00440	1/m	Column upper section: curvature in correspondence with $F_{y,n1}$

3.3 Results from experimental tests on the infilled portals F_{t1} and F_{t2}

The same cyclic test, previously performed on the bare portal, was performed on two prototypes both infilled with previously tested masonry: portals F_{t1} and F_{t2} .

During those tests the following damage, on the infill panel and on the frame itself, resulted:

1-Diagonal cracking: when the tensile strain and stresses (transverse to the principal compression stresses formed across the diagonal of the infill) exceed the masonry's cracking strain, diagonal cracking occurred starting from the center of the panel; as the interstory drift increased they extended diagonally from one corner to the opposite one;

2-Corner compression: as predictable in masonry characterized by strong bricks, due to the high stress concentrations of the compression diagonal in each corner, corner compression occurred. Corner crushing took place over a region limited to 2-3 bricks layers; the damage then extended into the concrete frame itself.

Corner crushing for the most part affected the upper corners, probably because the stiffer foundation beam caused a greater contact length. Therefore, this investigation considers the first story only. This is useful because experimental and numerical research in this field has shown, that infill (in-plane) damage tends to concentrate in the first few stories.

3-Bed-joint sliding: this behavior mode occurred in conjunction with the corner compression failure. This behavior was predictable because the mortar beds were relatively weak compared to the adjacent masonry; the plane of weakness formed near the higher part of the infill panel;

4-Shear yielding: when corner crushing occurred, the diagonal compression strut moved

downward into the column causing a large shear force at the extremity of the column. This led to large localized shear deformations at the top of the column.

As widely discussed in literature, the behavior modes previously described are ductile (shear yielding is not ductile but this behavior mode occurs after *corner compression* that is moderately ductile), in particular bed-joint sliding is associated with a high level of ductility while diagonal cracking and corner compression are associated to a moderate level of ductility (ref. *FEMA 306*).

Test on F_{t1}

Similar to F_{n1} , the first cracks appeared at the bottom of columns in correspondence to an approx. 4 mm horizontal displacement (interstory drift of 0.16%). Top displacement increased these cracks, decisively smaller than those found on F_{n1} , causing them to extend to approximately half the column's height but remained superficial: no plastic mechanism was observed at this stage.

With the increase of cycle magnitude, the infill panel started to detach from the surfaces of the columns and a resistant wall mechanism, associated to a diagonal compressed strut, became evident. The extent of the contact area between the wall and the column was measured progressively and a value of approximately 250 mm (this value corresponds to the one obtained with the Klinger and Bertero formula, 1976) was reached when a diagonal strut (diagonal compressed strut in the wall) developed, while the masonry remained intact. Achieving a top displacement of 10 mm, the cracks on the wall became very important and a consistent part of the bricks, at the corners, started to break and fell down.

When the maximum load was reached (top displacement of 18.7 mm), the bricks at the corners were severely damaged (crashing of the corners), and simultaneously, a horizontal sliding of the panel in correspondence to the third mortar layer from the top was observed.

As soon as bricks crushed, the load was fully absorbed by the columns, the first plastic hinges developed at the top of columns, and the structure collapsed.

As previously mentioned, the experimental data acquired by the transducers was lost due to technical problems. Results presented in the following report were evaluated starting with the information acquired from the M_h jack. Therefore no data from transducers was registered to evaluate the real displacements of the single frame (the deformation acquired by the jack is affected by the elastic deformation of the steel profile that links the frame to the jack); the loads can be considered real. For this purpose, the analyses described in the conclusive chapter of this paper will refer to results achieved by the tests performed on portals F_{n1} and F_{t2} .

Test on F_{t2}

Experimental test results on portal F_{t2} have shown a behavior comparable to portal F_{t1} although some differences were observable.

In fact in this second test the first cracks appeared at the upper half of the columns. The masonry crack pattern highlighted a well outlined compressed diagonal strut behavior and, also in this case, a strut dimension of approximately 250 mm was measured physically (the distance between the two parallel diagonal cracks observed at maximum load). As opposed to F_{t1} , brick crashing did not concentrate in exact correspondence to the corners: this may be justified by observing that bed-joint sliding occurred before the maximum strength of the compressed masonry was achieved, interrupting the diagonal strut continuity. As soon as the compressed diagonal strut crashed, the columns collapsed, the same as in F_{t1} .

Fig. 24 illustrates the trend of the column section curvatures: the lower one remained within the

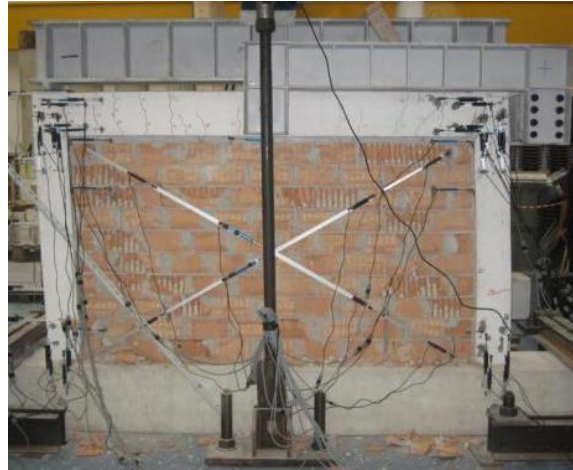


Fig. 18 Portal F_{11} : damage at the maximum load

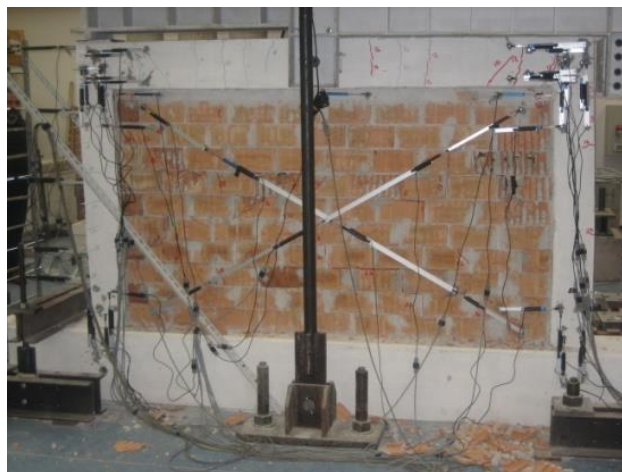


Fig. 19 Portal F_{12} : damage at the maximum load



Fig. 20 Portal F_{11} : masonry crushing damage (left) and portal collapse (right)



Fig. 21 Portal F_{12} : masonry crushing damage (left) and portal collapse (right)

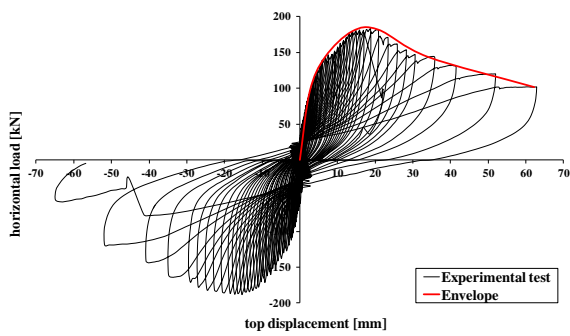


Fig. 22 Portal F_{11} , top displacement-horizontal load

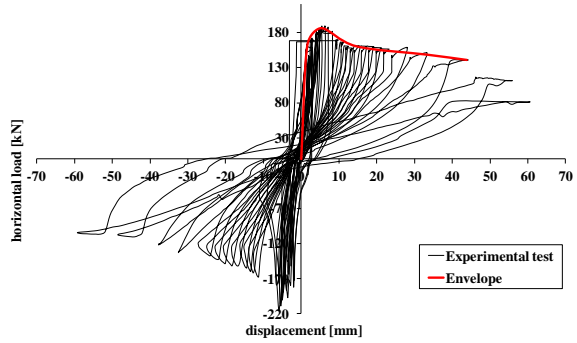


Fig. 23 Portal F_{12} , top displacement-horizontal load

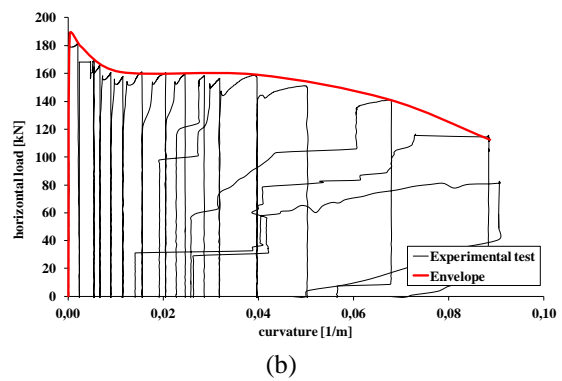
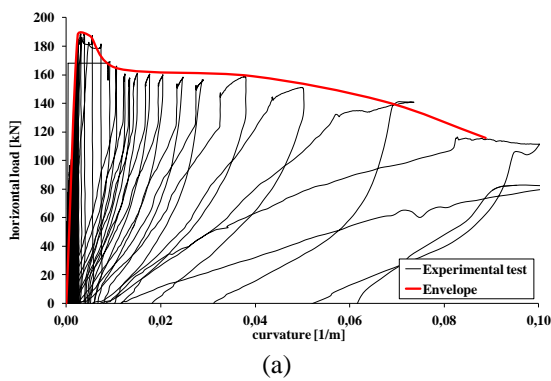


Fig. 24 Portal F_{12} column curvature-horizontal load: (a) lower section, (b) upper section

elastic range while the upper one registered important curvatures and the first plastic hinge formed before achieving the maximum horizontal load $F_{max,12}$. Fig. 25 illustrates the drift between the beam and the wall: this is the consequence the sliding between the beam and the higher bed-joint

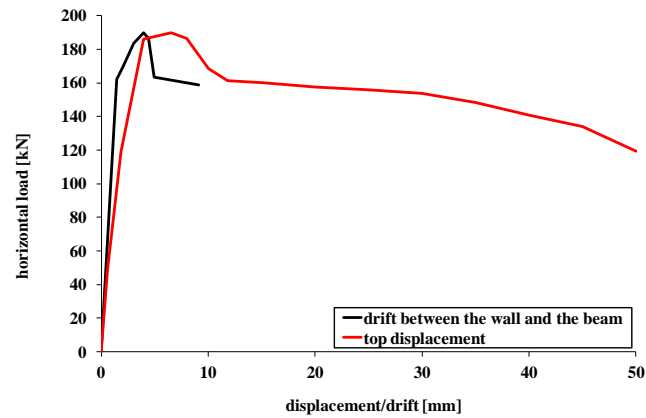


Fig. 25 Envelope of the drift between the upper layer of the masonry wall and the beam, during the experimental test

and highlights the development of this disconnection (this bed-joint is without load and therefore the friction is very low) during the progressive crushing of the masonry corners. As long as corners are intact the drift is linear whereas, as soon as the compressed strut loses stiffness and therefore the congruent behaviour of wall and frame is lost, the drift increases with a behaviour similar to the global loss of stiffness of the infilled frame.

4. Experimental determination of the equivalent strut

Since the studies performed by Klingner and Bertero (1976) non-linear analyses of infilled frames have usually been performed by replacing each individual panel with two or more diagonal struts using the uniaxial compressive law. A model proposed by Comberescue (1996) introduced a behavior law for a single truss element able to reproduce phenomena such as: stiffness degradation due to cracking, development of plastic strain and softening due to crushing and pinching associated with sliding (the strut has no tensile strength and the stress-strain curve under monotonic compressive loading is multilinear). Compressive strength degradation under cyclic loading is also measured by multiplying the plastic strain force to a factor which is a function of the cumulated cyclic plastic displacement. This behavior law is used only to predict the behavior of the monotonic line. To be defined, the behavior needs to be broken down into four branches: cracked behavior, stiffness decrease due to cracking, crushing of the diagonal strut and strength softening after crushing. In this study the equivalent single strut model was refined following the execution of the experimental tests with the intention of matching initial stiffness, plastic behavior, maximum strength and residual strength as much as possible. In the experimentally calibrated model the transition between the four branches of the Comberescue skeleton curve were determined by subtracting the F_{n1} capacity curve (that is the envelope of the cyclic test) from the F_{n2} capacity curve; with this procedure the trend of the horizontal load that was absorbed by the infill was estimated (this can be considered valid assuming that the r.c. structure will have an equivalent behavior, expressed by the capacity curve, in both configurations: bare or infilled). This approximation can be considered valid because of the absence of upper columns and lateral beams converging to the joints: the frame columns now experience increased axial forces but with

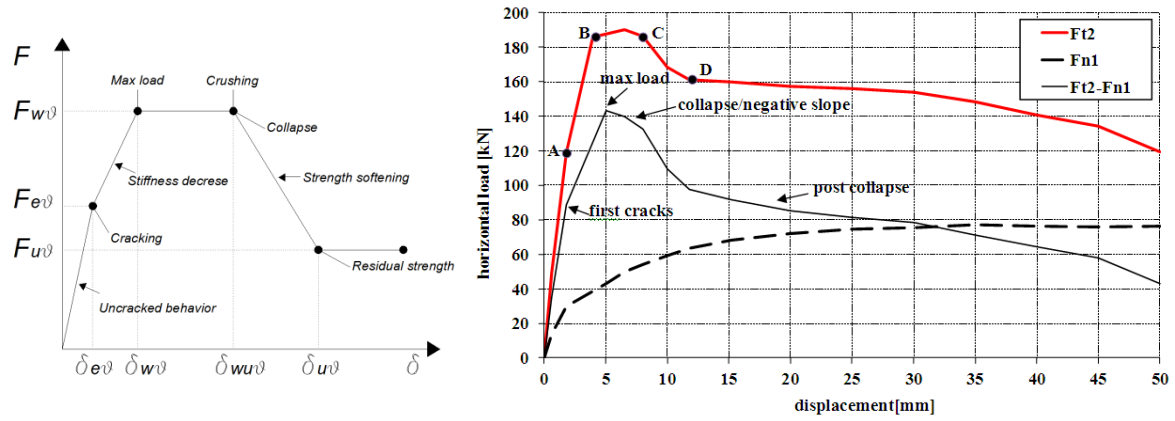


Fig. 26 Skeleton curve as proposed by Comberscuc (right). Characteristics of the equivalent strut determined as difference between the capacity curves of the portal F_{n1} and F_{t2} (left): A,B,C and D correspond, on F_{t2} curve, to cracking, max load, crushing/collapse and residual strength of masonry

Table 7 data from test on F_{t2}

Top displacement [mm]	Horizontal load [kN]	Infill condition
1.8	118.8	point A
4.16	186.1	point B
8.0	186.0	point C
12.0	161.5	point D

Table 8 experimental evaluation of the strut (distance from the two main diagonal cracks)

b_w =strut width	Dimension [mm]
Experimental	247.6 mm
Theoretical: Klingner and Bertero (1976)	254 mm

Table 9 load-deformation curve of the experimental strut model experimentally refined. The point ($d_{u\theta}$; $F_{residual}$) has been obtained imposing the slope of the softening branch (the same slope of the first part of the negative-slope range). In this table points A,B,C,D are expressed in terms of axial deformation and axial load (the axial direction is the corner to corner direction of the equivalent strut)

Load-deformation curve of the experimental strut			
Corresponding point (rif. Fig. 26 F_{t2} curve)	Deformation [mm]	Axial load [kN]	
	-	0	0
A	$d_{e\theta}$	1.68	$F_{e\theta}$ 102.2
B	$d_{w\theta}$	4.87	$F_{w\theta}$ 165.8
C	$d_{wu\theta}$	5.70	$F_{u\theta}$ 165.8
D	$d_{u\theta}$	40.61	$F_{residual}$ 30.00

reduced bending moments (Murty and Jain 2000). The capacity curves with their arithmetical differences, as well as the Comberscuc curve skeleton are plotted in Fig. 26; Tables 7-8 summarize

all significant data. The characteristics of the basic masonry model assigned to the strut in the non linear numerical frame models, developed with OpenSees software, are illustrated in Tables 9-11. The numerical analysis will be discussed in the following chapter.

The characteristics of the equivalent strut inserted in a numerical model (e.g., using a nonlinear link element) are described in Fig. 27: the relationship proposed is expressed in terms of axial resistance (load along the diagonal direction of the strut) and axial displacement (shortening of the strut element). Of course, if the strut is modeled using a frame element with an assigned area section, the same relationship can be expressed in terms of stress and strains in order to obtain the constitutive law of the strut material. In general, while the masonry’s mechanical characteristics can be identified through specific tests (i.e., the tests presented in the first part of this paper), an evaluation of the equivalent strut element’s characteristics remains extremely uncertain. The first uncertainty consists in the inability to determine the strength to be allocated to masonry that is compressed in an angle of θ and confined by both the surrounding masonry (the real wall is larger

Table 10 stress-strain curve (obtained considering a strut section of 200×247.6 mm and a strut length of 2640 mm) of the calibrated strut model refined experimentally; this is the constitutive law used in the nonlinear model (material of the strut element)

<i>Stress-strain curve of the calibrated strut model</i>			
<i>Corresponding point</i>	<i>e [-]</i>	<i>s [MPa]</i>	
A	0.06%	2.04	<i>Crack</i>
B	0.18%	3.31	<i>Max</i>
C	0.21%	3.31	<i>Failure</i>
D	1.50%	0.6	<i>Residual</i>

Table 11 summary of parameters of the refined model with ($E_i = s_A/e_A$; $E_c = s_B/e_B$; $K_s = F_{e\theta}/d_{e\theta}$)

E_i [MPa]	3433	<i>elastic modulus calculated on the first branch (branch 0-A)</i>
E_c [MPa]	1041	<i>cracked modulus calculated on the second branch (branch A-B)</i>
K_s [N/mm]	60833	<i>strut axial stiffness (branch 0-A)</i>

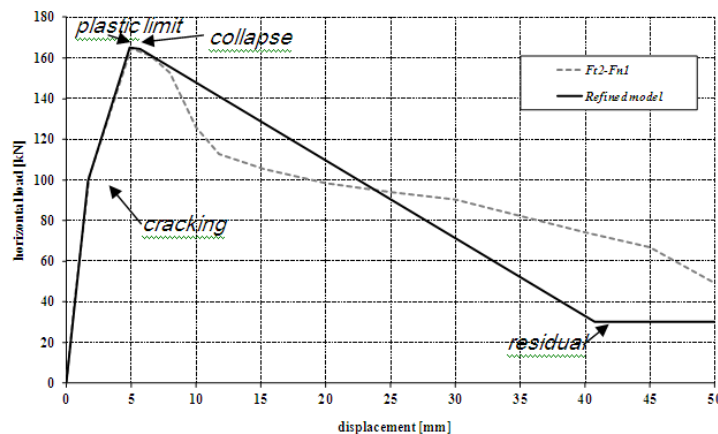


Fig. 27 Experimental results vs. The theoretical and calibrated model (implemented in the numerical model) of the diagonal strut, axial load-deformation

Table 12 Comparison of the stiffness of the infilled and bare frames tested

<i>Comparison between F_{n1} and F_{t2}</i>			
<i>Range</i>	<i>Stiffness</i> k_{Fn1} [kN/m]	<i>Stiffness</i> k_{Ft1} [kN/m]	<i>Ratio</i> [k_{Ft1}/k_{Fn1}]
0-A	16.6	66.0	3.9
A-B	5.4	28.5	5.2
B-C	2.8	0	0
C-D	2.4	-6.15	-2.5

than the samples) and the frame. From the refined model one can see, in this case, that the strength to be allocated to the diagonal strut is equivalent to 3.3 MPa (Table 10) that is approximately equivalent to the average value of compression strength f_w , evaluated using data considered reliable from Tables 1, 2, 3. The second uncertainty is the shear strength of the wall along the bed-joint; sliding between the bricks along the bed-joints influenced the resistance of both portals F_{t1} and F_{t2} . Since no experimental tests were performed on walls to determine this parameter, it wasn't possible to forecast how this could have affect the results. It was observed that infill sliding is responsible for the absence of a real plastic branch (horizontal segment when the maximum force is reached): this is considered to be the main uncertainty of a strut model. If experimental observations confirm the theoretical value of the strut's width, as per Klinger & Bertero's formula (Table 8), and once the size of the equivalent strut is defined, then a material approximately as strong as the average resistance from compression tests on wall samples, can be assigned to this type of masonry.

In Table 12, we compare some characteristics of the hysteretic response of the tested frame: the stiffness of the infilled frame k_{Ft1} , when compared to the bare frame k_{Fn1} , is 4 times higher in the undamaged masonry (range 0-A), upon masonry cracking the stiffness of the infilled frames decreases but the contribution of the cracked r.c. is even higher and therefore the ration k_{Ft1}/k_{Fn1} increases. In fact passing over to point A the stiffness decrease is 67% for the bare frame and 57% for the infilled one: therefore the contribution to stiffness can be considered significant until point B. After this stage the contribution to the global resistance is still relevant but the stiffness of the damaged wall is compromised.

5. Comparison of experimental and numerical results

Results of the experimental tests were compared with the analyses performed on numerical models implemented with the use of OpenSees fibre based elements: the masonry was modelled using the previously described refined equivalent single strut element. The following Figs. 28-29 compare results from numerical analyses and experimental tests. As one can see, the numerical models of the bare and infilled portal appear to be well calibrated. The estimated stiffness coincides both with the experimental stiffness and the value of maximum horizontal load.

The experimental results highlight a dissymmetry, the positive load developed is slightly higher than those measured in the opposite thrust direction. The numerical model is perfectly symmetrical and has a trend closer to the experimental measurements of the negative load values (jack contraction). This can be explained by observing that the portal prototype, as well as the linking

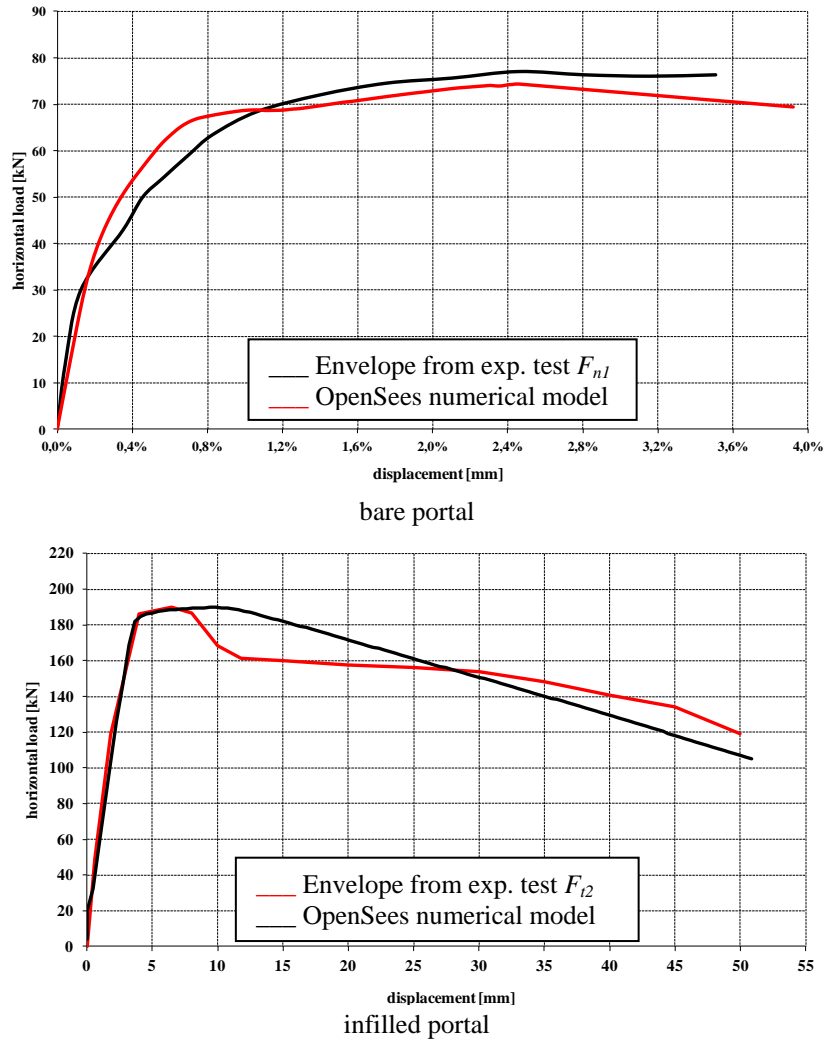


Fig. 28 Envelope of the cycles (x direction) experimental and numerical capacity curves

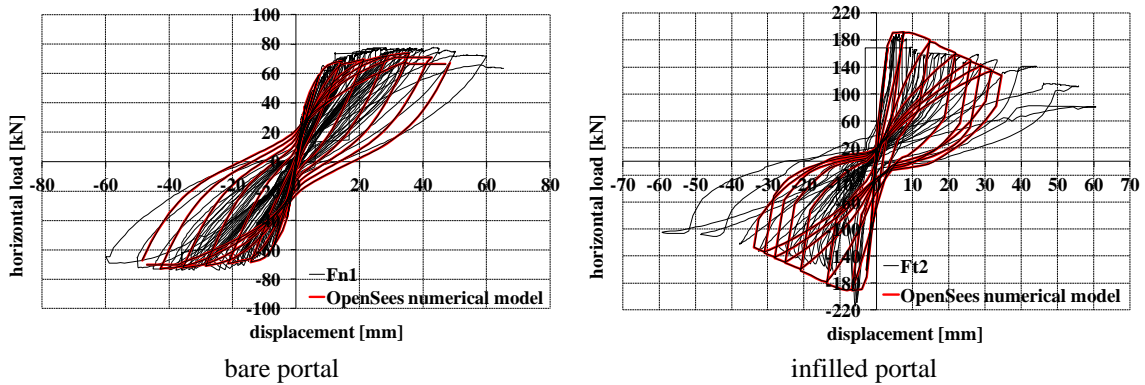


Fig. 29 experimental (black line) and numerical cyclic analysis (red line)

structure between the jack and the portal, were not perfectly geometric. The structure therefore felt, the effects of a load eccentricity: in the jack extension phase a slight strain of the compressed linking profile increased the existing eccentricity thus affecting the final result. Therefore one can correctly consider more reliable the load measured during the contraction of the jack (in this condition the linking element is firm).

However, with regard to the activities carried out on the bare and infilled portals, both the experimental and numerical results have been presented. One can observe that the numerical model developed using an experimentally calibrated single strut element, developed according to Comberescue's skeleton curve, well represents its global behavior in terms of elastic stiffness, maximum resistance, post yielding stiffness and ductility.

6. Conclusions

This paper, part of a broader research project, relates to an experimental investigation on the behavior of reinforced concrete frames, designed without seismic detailing (as per outdated Italian technical code DM 1996).

Three reinforced concrete one-bay one-story frame specimens, one bare and two infilled, were made on a scale ratio of 1:2 and were tested under constant vertical and in-plane cyclic lateral loads. In particular, when testing the infilled prototype, it was observed that in the masonry panel, the first crack occurred at drift of about 0.05%, reaching maximum capacity at drift of about 0.5% while retaining its capacity up to a drift of 0.6%. The framed masonry lost its composite action precisely when shear stress reached shear friction on the masonry-concrete interface. Infill contributed to the stiffness and strength of the bare reinforced concrete frame at small drifts thus improving overall system behavior.

The damage concentrated at the masonry infill and could be divided into three main ranges: up to a drift of 0.25%, there was no damage and the system behaved almost elastically; in drifts from 0.25%-0.35%, infill contribution lessened, and damage to the infill increased; in drifts from 0.35%-0.6%, there was no increase in the overall lateral capacity, and damage to the infill was repairable; over a drift of 0.6%, infill was heavily damaged. Infill contribution is neglectable in further drifts. Infill contribution to the overall structural performance is significant because it enhances stiffness and strength. This can modify the overall structural performance in terms of load distribution, stiffness distribution and can therefore influence collapse behavior and modal shapes. The presence of the infills can determine deformation concentration in one floor (soft story), concentration of forces on elements (concentration of shear action on columns) and, if compared with what can be predicted if considering the single structural frame, a different seismic action. Existing global models for masonry infill panels, such as the equivalent single strut element, can be easily adopted for infilled frames but, while they perform well in terms of building global behavior, they poorly represent some experimentally observed mechanisms (shear concentration on column extremities, bed-joint sliding, corner crushing); further developments are needed here. The possibility of including masonry infills in the design or analysis of new and existing buildings could be exploited by considering the framed infill as a structural element. The importance of this approach is confirmed by the experiences encountered after seismic events as well as during the experimental activity. According to the results obtained in this research a constitutive load, formed by 5 branches (elastic, stiffness decay, plastic, softening and residual), like the one proposed by Comberescue, could well represent the masonry panel's real behavior.

However a calibration procedure, defining the transition points between one branch and the others and based only on some elemental tests is difficult to identify. According to the results of this research and the specific characteristics of the masonry wall, we suggest what follows: the strength allocated to the diagonal strut should be approximately equivalent to the average value of the compression strength determined on the wall samples from tests executed diagonally, parallel and orthogonal to the holes. The author suggests that during the execution of these tests results substantially different from the others should not be included in the calculations: many conditions that are difficult to notice during the preparatory phase could alter the results. If experimental observations confirm the theoretical value of the contact length, and once the size of the equivalent strut is defined, then a material approximately as strong as the average resistance determined from the three typologies of compression tests on wall samples (horizontal, vertical and diagonal tests), can be assigned to this type of masonry.

References

- Active Standard ASTM E519/E519M Standard Test Method for Diagonal Tension (Shear) in Masonry Assemblages, Developed by Subcommittee: C15.04. Book of Standards **04, 05**.
- Bergami, A.V. (2011), "Masonry infilled r.c. frames Implementation and experimental verification of models for nonlinear analysis", *LAP LAMBERT Academic Publishing GmbH & Co. KG*, ISBN: 978-3-8465-0324-9.
- Bergami, A. and Nuti, C. (2015), "Compression tests on masonry walls realized with a single or double masonry panel", *J. Civ. Eng. Arch. Res.*, **2**(7).
- Colangelo, F. (2005), "Pseudo-dynamic seismic response of reinforced concrete frames infilled with non-structural brick masonry", *Earthq. Eng. Struct. Dyn.*, **34**(10), 1219-1241.
- Combescur, D. (1996), "Modélisation du comportement sous chargement sismique des structures de bâtiment comportant des murs de remplissage en maçonnerie", PhD. Thesis, Ecole Centrale Paris, France.
- D.M.LL.PP. del 20/11/1987, Norme tecniche per la progettazione, esecuzione e collaudo degli edifici in muratura e per il loro consolidamento (Italian masonry code).
- D.M.LL.PP. del 09/01/1996, Norme tecniche per il calcolo, l'esecuzione ed il collaudo delle strutture in cemento armato, normale e precompresso e per le strutture metalliche (Italian technical code).
- Federal Emergency management Agency (1998), "Evaluation of earthquake damaged concrete and masonry wall buildings, basic procedures manual", ATC-43, FEMA 306, ATC, California.
- Fardis, M.N., Bousias, S.N., Franchioni, G. and Panagiotakos, T.B. (1999), "Seismic response and design of RC structures with plan-eccentric masonry infills", *Earthq. Eng. Struct. Dyn.*, **28**(2), 173-191.
- Klingner, R.E. and Bertero, V.V. (1976), "Infilled frames in earthquake-resistant construction", Report No. EERC 76-32, University of California, Berkeley.
- Klingner, R.E. and Bertero, V.V. (1976), "Infilled frames in earthquake resistant construction", Report 76-32, University of California, Berkeley, USA.
- Mainstone, R. (1971), "On the stiffness and strength of infilled frames", *Proceedings of the Institution of Civil Engineers, Supplement*, **48**, 57-90.
- Mehrabi, A.B., Shing, P.B., Schuller, M. and Noland, J. (1996), "Experimental evaluation of masonry-infilled RC frames", *J. Struct. Eng.*, ASCE, **122**(3), 228-237.
- Murty, C.V.R. and Jain, S.K. (2000), "Beneficial influence of masonry infills on seismic performance of RC frame buildings", *Proceedings 12th World Conference on Earthquake Engineering*, New Zealand.